CELL CYCLE
2019, VOL. 18, NOS. 6–7, 670–681
https://doi.org/10.1080/15384101.2019.1578144

Taylor & Francis
Taylor & Francis Group

RESEARCH PAPER

Up-regulation of THY1 attenuates interstitial pulmonary fibrosis and promotes lung fibroblast apoptosis during acute interstitial pneumonia by blockade of the WNT signaling pathway

Lin Chen[a*], Rong-Zhen Tang[b*], Jia Ruan[c], Xiao-Bo Zhu[d], and Yang Yang[a]

[a]Department of Respiratory and Critical Care Medicine, Sichuan Academy of Medical Sciences & Sichuan Province People's Hospital, Chengdu, P.R. China; [b]Department of Aged Infectious Diseases, Sichuan Academy of Medical Sciences & Sichuan Province People's Hospital, Chengdu, P.R. China; [c]Department of Respiratory Diseases, Sichuan West China Hospital Geriatric Center-Fifth People's Hospital of Sichuan Province, Chengdu, P.R. China; [d]Department of Respiratory Diseases, Ziyang City People's Hospital, Ziyang, P.R. China

ABSTRACT

Acute interstitial pneumonia (AIP) is an idiopathic pulmonary disease featuring rapid progressive dyspnea and respiratory failure. These symptoms typically develop within several days or weeks in patients without any pre-existing lung disease or external chest disease. Thymocyte differentiation antigen-1 (THY1) has been reported to have an effect on lung fibroblast proliferation and fibrogenic signaling. In this study, the mechanism of THY1 in AIP in influencing pulmonary fibrosis in terms of lung fibroblast proliferation and apoptosis was examined. An AIP mouse model with the pathological changes of lung tissues observed was established to identify the role of THY1 in the pathogenesis of AIP. The expression of THY1, a key regulator of the WNT pathway β-catenin and fibroblasts markers MMP-2, Occludin, α-SMA and Vimentin were determined. Lung fibroblasts of mice were isolated, in which THY1 expression was altered to identify roles THY1 plays in cell viability and apoptosis. A TOP/TOPflash assay was utilized to determine the activation of WNT pathway. Decrement of pulmonary fibrosis was achieved through THY1 up-regulation. The expression of MMP-2, Occludin, α-SMA, Vimentin and β-catenin, and the extent of β-catenin phosphorylation, significantly decreased, thereby indicating that THY1 overexpression inactivated WNT. Cell proliferation was inhibited and apoptosis was accelerated in lung fibroblasts transfected with vector carrying overexpressed THY1. Altogether, this study defines the potential role of THY1 in remission of AIP, via the upregulation of THY1, which renders the WNT pathway inactive. This inactivation of the WNT signaling pathway could alleviate pulmonary fibrosis by reducing lung fibroblast proliferation in AIP.

Abbreviations: AIP: Acute interstitial pneumonia; ILDs: interstitial lung diseases; DAD: diffuse alveolar damage; SPF: specific-pathogen-free; NC: negative control; HCMV: human cytomegalovirus; HE: Hematoxylin-eosin; RIPA: radio-immunoprecipitation assay; SDS-PAGE: sodium dodecyl sulfate-polyacrylamide gel electrophoresis; BSA: bovine serum albumin; HRP: horseradish peroxidase; ECL: electrochemiluminescence; FBS: fetal bovine serum; DMSO: dimethyl sulfoxide; OD: optical density

ARTICLE HISTORY
Received 30 July 2018
Revised 30 November 2018
Accepted 12 December 2018

KEYWORDS
Thymocyte differentiation antigen-1; WNT signaling pathway; acute interstitial pneumonia; pulmonary fibrosis; lung fibroblast; proliferation

Introduction

Interstitial lung diseases (ILDs) are a group of pulmonary parenchymal diseases characterized by analogous clinical, physiologic, radiologic, and pathologic manifestations [1]. Acute interstitial pneumonia (AIP), also called Hamman-Rich syndrome, is a rarely occurred idiopathic ILD featured with rapid progressive respiratory failure and high mortality [2]. Myofibroblasts are essential to the progression of diffused alveolar damage (DAD), which is a key characteristic of AIP [3]. AIP can affect patients of any age or gender, and is often preceded by an upper respiratory tract infection marked by fatigue and myalgia [4]. The prognosis of AIP seems to be pessimistic with a death rate > 50% after the onset of AIP in the first 2 months [2]. Therefore, it is of great importance to further understand the mechanisms and pathogenesis of AIP to develop more effective therapeutic strategies.

Gene expression is one of the most fundamental processes of life, including the transcription,

CONTACT Lin Chen chenlinhx@med.uestc.edu.cn
*These authors contributed equally to this work.

translation and turnover of messenger RNAs (mRNAs) and proteins [5]. Thymocyte differentiation antigen-1 (THY1) is a highly conserved glycoprotein belonging to the immunoglobulin superfamily [6]. THY1, also known as CD90, has been previously demonstrated as a cancer biomarker [7]. THY1 is known as a glycoprotein as well as an indicator of cancer stem cells (CSC) and it's upregulation has been found in lung malignancies [8,9]. It was revealed that THY1 could bind to integrins in different tissue contexts to regulate the cellular interaction and it could serve as biomarker for the treatment of human lung cancer [10]. THY1 has also been shown to be expressed differently in endothelial cells, neuronal cells and fibroblasts [11]. Previous studies have shown that the overexpression of THY1 contributes to the inhibition of anchorage-independent growth *in vitro*, and tumor formation *in vivo* [12]. Previous studies have that the absence of THY1 can induce a higher susceptibility to pulmonary fibrosis in mice [13]. Moreover, the osteogenic capability can be enhanced via the THY1-positive selection [14]. Furthermore, previous studies have found the expression of THY1 in prostate cancer-associated fibroblasts to be intense [15]. Additionally, aberrant WNT signaling pathways, which are closely associated with cancer, have been shown to have an effect on maintaining cancer stem cells, metastasis and immune control [16]. Previous studies have proposed that inactivation of WNT signaling pathway could function as a tumor suppressor [17]. The WNT signaling pathway has emerged as a critical regulator which widely impacts biological aspects involved in lung development [18]. The transcription of WNT targets gene regulated by nuclear β-catenin [19]. Chen *et al.* revealed that WNT was involved in the regulation of cancer-associated fibroblasts on cancer stem cells (CSC)-like characteristics in lung CSC [20]. At the same time, activated WNT signaling pathway is a common feature of fibrotic disease and can strongly stimulate fibroblast activation and tissue fibrosis including pulmonary fibrosis [21]. However, the mechanism of THY1 that is involved with the WNT signaling pathway in AIP is still under investigation. Therefore, in this study, whether the overexpression of THY1 could influence pulmonary fibrosis and lung fibroblast proliferation in AIP through interaction with the WNT signaling pathway was tested.

Results

Mouse model of AIP is successfully established

According to the observation results (Table 1), the respiratory rate of mice, as well as the positive rate of immunoglobulin M (IgM) and immunoglobulin G, (IgG) was increased. However, the weight was decreased in the NC, AIP and THY1 vector groups when compared to that of the mice in the normal group (all $p < 0.05$). These findings demonstrated that the mouse model of AIP was successfully established.

Overexpression of THY1 reduces pulmonary fibrosis

The pathological morphology of lung tissues was observed using HE staining and Masson staining under an optical microscope. When compared to those of the normal group, the lung tissues of mice in the NC, AIP and THY1 vector groups were swollen with an irregular appearance and existence of scars, indicating pulmonary fibrosis (Figure 1). In addition to pulmonary fibrosis, the alveolar structure in the other three groups was damaged according to the results from the Masson staining (Figure 2). Disordered structure of the alveolar epithelium, the reduction of alveolar cavity area and thickening of the alveolar wall were all observed (Figure 2). Moreover, lung interstitium was progressively replaced by fibrous connective tissue, and diffused pulmonary fibrosis occurred in lung tissues. However, scars, pulmonary fibrosis, and collagen fiber deposition in the lung tissue in the THY1 vector groups were distinc-

Table 1. The respiratory rates, weights and immunoglobulin positive rate of mice in each group.

Group	Respiratory rate (min)	Weight (g)	IgM positive rate (%)	IgG positive rate (%)
Normal	129.25 ± 11.92	23.17 ± 2.15	0.00	16.70
AIP	153.33 ± 16.08*	16.33 ± 1.43*	66.70*	83.30*
NC	161.50 ± 17.02*	17.33 ± 1.49*	75.00*	75.00*
THY1 vector	183.50 ± 14.92*	16.75 ± 1.59*	58.30*	50.00*

AIP, acute interstitial pneumonia; IgM, immunoglobulin M; IgG, immunoglobulin G; *, $p < 0.05$ *vs.* the normal group.

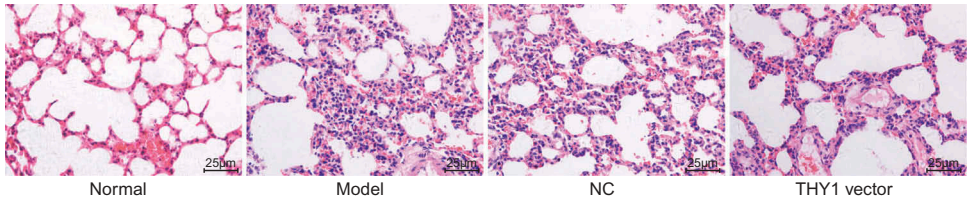

Figure 1. THY1 overexpression contributes to the reduction of pulmonary fibrosis detected by HE staining (400 ×). THY1, thymocyte differentiation antigen-1; HE, hematoxylin-eosin; AIP, acute interstitial pneumonia; NC, negative control.

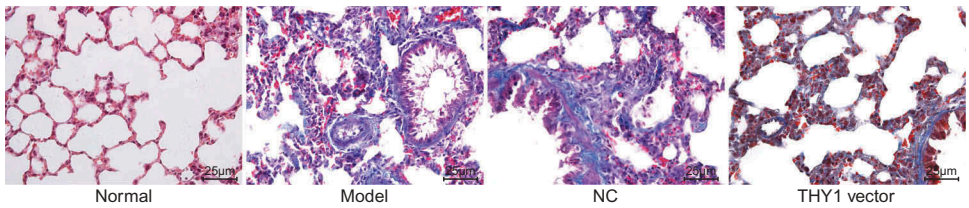

Figure 2. Up-regulation of THY1 reduces pulmonary fibrosis revealed by Masson staining (400 ×). THY1, thymocyte differentiation antigen-1; AIP, acute interstitial pneumonia; NC, negative control.

tively less severe when compared to those of the NC and AIP groups. Furthermore, when the lung tissue of the THY1 vector group was observed, the alveoli were found to be more intact, the pulmonary alveolar area was found to be enlarged, the alveolar wall was thinned, alveolar inflammation was slightly changed, alveolar wall destruction declined, fibrosis was mild, and pulmonary fibrosis was found to be alleviated. All of the above observations showed that the decrement of pulmonary fibrosis could be achieved through THY1 up-regulation.

THY1 overexpression inactivates the WNT signaling pathway and downregulates fibroblasts markers

The detailed regulatory effects of THY1 on the WNT signaling pathway-related gene β-catenin and fibroblast markers MMP-2, Occludin, α-SMA, and Vimentin were all studied in lung tissues *in vitro* by using RT-qPCR and western blot analysis. As the results shown in Figure 3(a-c), when compared to that of the normal group, the THY1 expression decreased in the NC and AIP groups and even in the THY1 vector group, where a significant increment of mRNA and protein expression of MMP-2, Occludin, α-SMA, Vimentin, β-catenin, as well as the extent of β-catenin was observed (all $p < 0.05$). However, the expression of THY1 was increased while the mRNA and the protein levels of MMP-2, Occludin, α-SMA, Vimentin, β-catenin, as well as the extent of β-catenin were lowered in the THY1 vector group, when compared to those of the NC and AIP groups (all $p < 0.05$). No significant difference regarding the mRNA and protein expression of THY1, MMP-2, Occludin, α-SMA, Vimentin, β-catenin, as well as the extent of β-catenin was observed between the NC and AIP groups (all $p > 0.05$). These findings indicated that up-regulation of THY1 could induce inactivation of the WNT signaling pathway and downregulate fibroblasts markers.

TOP/FOPflash was widely recognized as an index for the activated WNT/β-catenin signaling pathway in cells. The critical point for activation of the WNT/β-catenin signaling pathway is that accumulated β-catenin enters the nucleus and binds itself to the TCF/LEF to regulate the gene expression. In this present study, it was found that, when compared to that of the normal group, the fluorescence activity of TOP/FOPflash in the NC and ALP groups was enhanced. However, the fluorescence activity of TOP/FOPflash in the THY1 vector group was inhibited in comparison with the NC and AIP groups ($p < 0.05$; Figure 3(d)). These findings further demonstrated that overexpressed THY1 could inactivate the WNT/β-catenin signaling pathway.

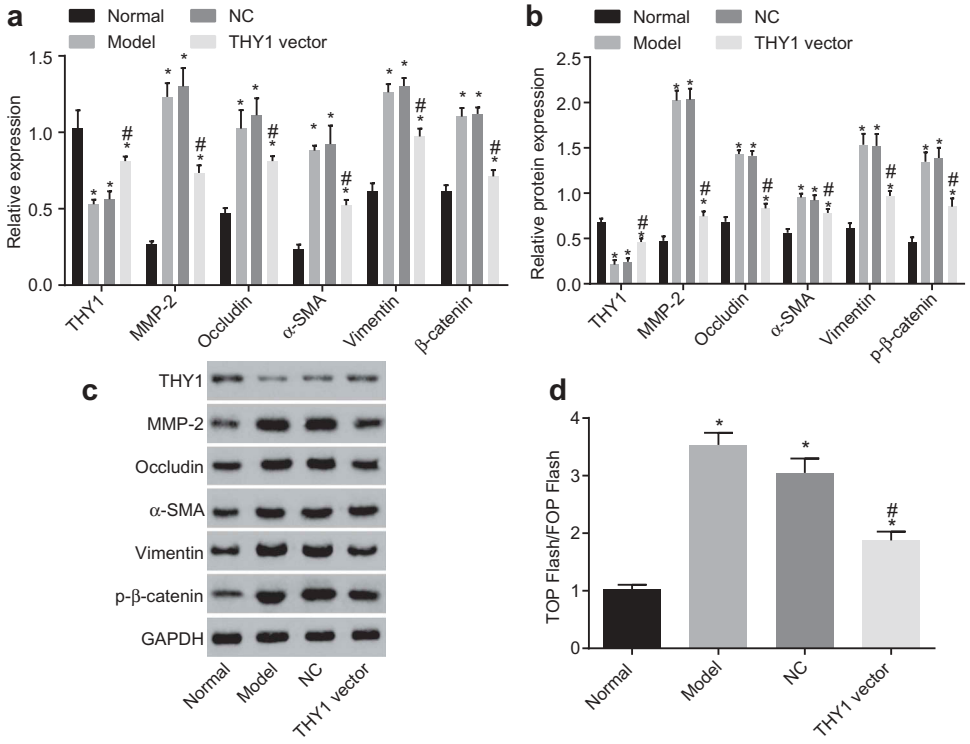

Figure 3. MMP-2, Occludin, α-SMA, Vimentin and β-catenin expression is suppressed by THY1 overexpression. (a), relative gene expression and mRNA levels of THY1, MMP-2, Occludin, α-SMA, Vimentin and β-catenin in lung tissues after transfection; (b) and (c), the protein expression of THY1, MMP-2, Occludin, α-SMA, Vimentin and the extent of β-catenin phosphorylation in lung tissues after transfection by western blot analysis; (d), luciferase activity in each group detected by TOP/FOPflash rassay; the data refer to the ratio of firefly luciferase activity to renilla luciferase activity; *, $p < 0.05$ *vs*. the normal group; #, $p < 0.05$ *vs*. the NC and AIP groups; THY1, thymocyte differentiation antigen-1; RT-qPCR, reverse transcription-quantitative polymerase chain reaction; MMP-2, matrix metalloprotein 2; α-SMA, alpha-smooth muscle actin; AIP, acute interstitial pneumonia; NC, negative control.

Morphological changes of pulmonary fibroblasts

Following detachment of pulmonary fibroblast cells, a 4-day-static-adherence cell growth observation period was held. Following this observation period, there were round-like cells crawling from the lung fibroblast tissues. Seven days later, cells were covered with the whole monolayer in palisading and radial arrangement. Cells were in long fusiform and cord-like shape after purified by differential centrifugation and different rates of attachment. Furthermore, when inoculating the cells that had been dissociated with trypsin, a large number of round-like cells grew by static adherence 2 d later. On the 5th day, cells were spindle or strip-like and reached a density of about 80% on the 7th day (Figure 4).

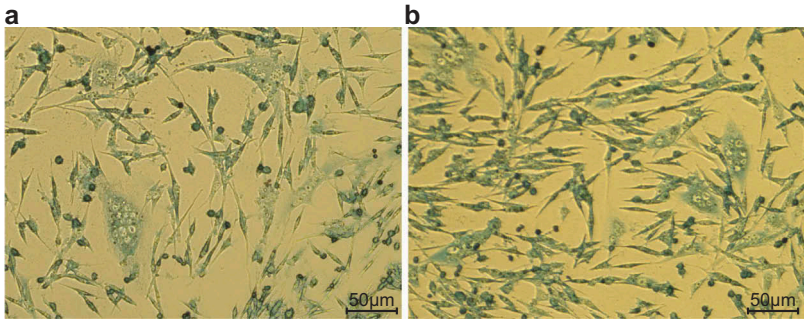

Figure 4. Morphology of primary lung fibroblasts in adult mice (200 ×). (a), mouse lung fibroblasts are round-like before separation and purification; (b), mouse lung fibroblasts are spindle or strip-like after separation and purification.

THY1 overexpression and WNT signaling pathway knockdown inhibit lung fibroblast proliferation

The MTT assay was adopted to measure the proliferation ability of lung fibroblasts. As indicated in Figure 5, cell proliferation was accelerated significantly in the NC, AIP and THY1 vector groups when compared to that of the normal group (all $p < 0.05$), while the THY1 vector group had the suppressed cell proliferation when compared with the NC and AIP groups ($p < 0.05$). No significant difference was found regarding to the cell proliferative ability between the NC and AIP groups ($p > 0.05$). The phenomenon demonstrated that cell proliferation of lung fibroblasts could be inhibited through the intense expression of THY1.

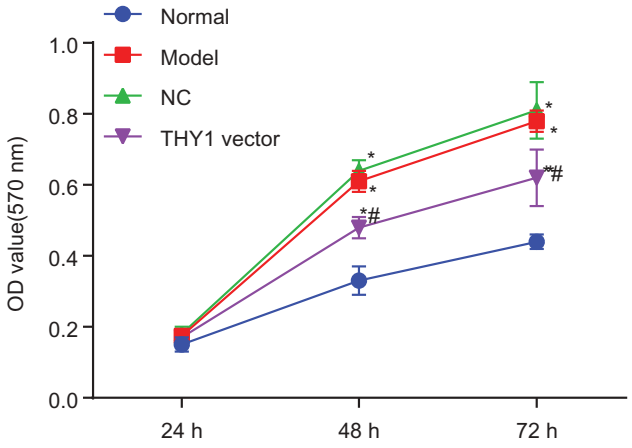

Figure 5. The MTT assay demonstrates that lung fibroblast proliferation is inhibited by the overexpression of THY1 and the inactivation of the WNT signaling pathway. *, $p < 0.05$ *vs*. the normal group; #, $p < 0.05$ *vs*. the NC and AIP groups; MTT, 3-(4,5-dimethylthiazol-2-yl)-2,5-diphenyltetrazolium bromide; THY1, thymocyte differentiation antigen-1; AIP, acute interstitial pneumonia; NC, negative control.

THY1 overexpression and WNT signaling pathway knockdown promote lung fibroblast apoptosis

According to the results of Annexin V-FITC/PI double staining (Figure 6) and detection by flow cytometry, when compared to that of the normal group, cell apoptosis was slowed down in the NC, AIP and THY1 vector groups (all $p < 0.05$). However, in contrast to the NC and AIP groups, a distinctive increment of apoptosis rate was found in the THY1 vector group ($p < 0.05$). No significance was found in terms of the apoptosis rate between the NC and AIP groups ($p > 0.05$). These findings provided evidence proving that lung fibroblast apoptosis could be enhanced through THY1 overexpression.

Discussion

AIP is a type of idiopathic interstitial pneumonia, whose pathogenesis remains unclear [22]. In

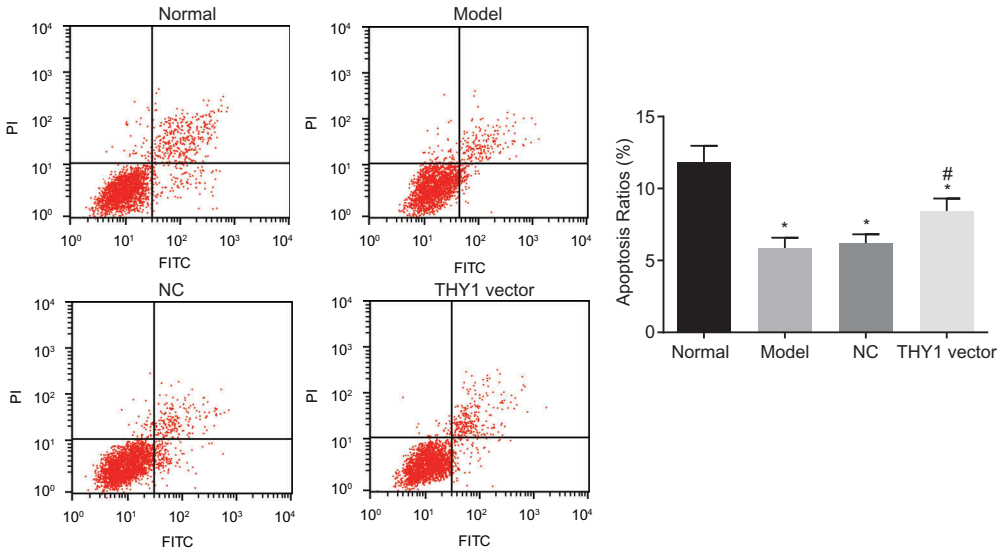

Figure 6. The Annexin V/PI double staining indicates that lung fibroblast apoptosis is promoted by THY1 up-regulation and WNT signaling pathway inactivation. *, $p < 0.05$ *vs*. the normal group; #, $p < 0.05$ *vs*. the NC and AIP groups; PI, propidium iodide; THY1, thymocyte differentiation antigen-1; AIP, acute interstitial pneumonia; NC, negative control.

addition, the diagnosis of idiopathic pulmonary fibrosis (IPF) and other ILD has been confronted with enormous clinical challenges [23]. It has been reported that pulmonary fibrosis usually manifests itself as a fibro-proliferative lung disease with an irreversible chronic progression and dismal prognosis [24]. THY1, with its expression on normal lung fibroblasts but absence in myofibroblasts within fibroblastic foci, is considered as a significant regulator of cell-cell and cell-matrix interactions in IPF [25]. Furthermore, the cardiac fibroblasts that are induced by CD90+ (THY1+) exhibit alleviated fibrosis in a rat model of acute myocardial injury [26]. In this study, the role of THY1 in AIP in relation to the WNT signaling pathway was presented, which showcased that THY1 blocks the WNT signaling pathway, and correspondingly regulates proliferation, apoptosis and interstitial pulmonary fibrosis in AIP.

To begin, it was found that lung fibroblasts exhibited decreased expression of α-SMA, Vimentin and β-catenin following treatment of THY1 overexpression, indicating that overexpression of THY1 inhibited the WNT signaling pathway. WNT signaling pathway was also found to be a potent fibrogenic growth factor released by activated alveolar epithelial cells and could recruit inflammatory cells during the initial injury phase conducive to the perpetuation of injury, repair failure and fibrosis cycle [27]. Moreover, a previous study has indicated that the potential anti-fibrotic effects in well-tolerated doses could be achieved through inactivation of tankyrases, which effectively inhibited the activation of canonical WNT signaling pathway [28]. Taking this information into account, the activation of WNT/β-catenin pathway in IPF lung tissues presented a β-catenin intense immunoreactivity, as well as a high expression rate of cyclin-D1 and matrilysin, all of which were downstream genes of the WNT/β-catenin pathway [29]. In addition to this, another study revealed that depleted β-catenin could not entirely suppress fibrosis development while the sustained accumulation of β-catenin in the cell was facilitating the expression of a fibrogenic program in fibroblasts by WNT signaling pathway [30]. A mouse model of pulmonary fibrosis that was induced by bleomycin exhibited decreased pulmonary fibrosis by inactivating the WNT/β-catenin pathway through short interfering RNA against β-catenin [31]. Furthermore, the WNT pathway has been widely reported to be correlated to the Hippo-yes-associated protein (YAP) signaling pathway and the WNT signaling pathway could mediate the expression of yap-1 transcriptionally [32]. In continuing with YAP, it has been revealed that YAP is associated with multiple signaling pathways, including the WNT/β-catenin signaling pathway [33]. In addition to this information, YAP is a main player in Hippo and both WNT and Hippo pathways participate in various cellular developments of many diseases [34]. It was recently demonstrated that the YAP mediated by E-cadherin could be included in the destruction complex of β-catenin in order to orchestrate WNT signaling [35]. In this study, experimental results were consistent with the aforementioned studies that the mRNA and protein levels of β-catenin were increased in AIP lung fibroblasts. When lung fibroblasts were transfected with THY1 overexpression plasmids, the pulmonary fibrosis was alleviated along with downregulation of β-catenin, which indicated the blockade of WNT signaling pathway. Exosomes refer to nanoparticles originating from viable cells and are widely found to exert effects on the intercellular communication with multiple biological functions in many disease [36]. It has been previously reported that exosomes derived from stromal fibroblasts could enhance the drug resistance to colorectal cancer [37]. Furthermore, adipose-derived stem cells could secrete exosomes, which in turn exhibit biological effects on tissue regeneration and could protect against tissues of bone, muscle, skin, and brain [38].

In addition, overexpression of THY1 could reduce levels of MMP-2 and Occludin, leading to inhibition of proliferation and enhancement of lung fibroblasts apoptosis by inactivating the WNT signaling pathway in AIP. As the first complete membrane protein in the endothelial cell tight junctions, Occludin directly determines the cell permeability of different ions or macromolecules, and recessive mutations in the gene encoding Occludin were proved to cause abnormal cortical development [39]. MMPs were the main enzymes implicated in degradation and

remodeling of extracellular matrix, and MMP-2 played a significant role in metastasis and invasion [40]. Previous studies have shown that THY1 positive-expressed CSCs might provide an ideal target for anti-angiogenesis treatment of gliomas [41]. Furthermore, similar studies have also revealed the crucial role THY1 plays in the development and progression of glioblastoma multiforme CSCs, which enlightened the further studies that THY1 might be an appropriate target for anti-tumor vasculature [42]. Not only does THY1 act as a candidate marker for cancer therapy but THY1 also is involved in cell adhesion, migration and fibrosis [6]. It was easier for fibroblasts to transform into myofibroblasts by positively expressing THY1, a versatile regulator of cellular processes [43]. Additionally, overexpression of THY1 could suppress lung fibroblast proliferation as well as lung fibroblast proliferation induced by lipopolysaccharide [44]. Moreover, a recent study also provided new evidence that overexpressed THY1 in lipid rafts and colocalization with Fas advanced apoptosis in lung fibroblast [45]. The evidence provides strong arguments that overexpression of THY1 can lead to a decrement of interstitial pulmonary fibrosis.

Given the experimental results that THY1 was down-regulated in AIP lung tissues in relation to the progression of AIP, and that the antifibrotic role of THY1 could be achieved through inactivation of WNT signaling pathway, a potential therapy target, THY1, for treatment of AIP is proposed. However, more detailed studies in representative models for fibrosis on gene and pathway expression are still required to completely understand the molecular cross-talk *in vivo*. Expanding knowledge on signal transduction will provide a better understanding on how a limited set of growth factors are able to govern the complex processes that underlie the physiology and pathology of fibrotic disorders.

Materials and methods

Ethics statement

The experimental procedures and animal-use protocols have been approved by the Animal Ethics Committee of Sichuan Academy of Medical Sciences & Sichuan Province People's Hospital. In addition, all animal experiments in this study were in accordance with the principles of management and use of local laboratory animals.

Study subjects

Forty eight specific-pathogen-free (SPF) BALB/c female mice (age: 10 wk; weight: 18 ~ 27 g; Experimental Animal Center of Xinjiang Medical University, Urumqi, Xinjiang) were housed individually at 25°C in the SPF-grade environment with relative humidity of 55% ~ 65% with free access to food and water for 1 wk before the experiment. The health condition of the mice was observed before the experiment.

Lentiviral vector construction and lentiviral package

The designed primers were amplified to obtain the full-length mouse THY1 gene. The THY1 target gene and p LVX-IRES-Zs Green 1 vector were cleaved at the restrictive endonuclease sites: Xho I and Bam H I. The large fragments of p LVX-IRES-Zs Green 1 vector and THY1 gene were collected and connected into competent cells of Escherichia coli using T4 ligase to construct the lentiviral expression vector of p LVX-IRES-Zs Green 1. Following the construction of the lentiviral expression vector, three helper plasmids, that were required for the construction of the recombinant plasmid and lentiviral package of p LVX-IRES-Zs Green 1, were co-transfected into human embryonic kidney (HEK)-293T cells for ST2 lentiviral package, followed by detection of tilter and activity of virus.

Model establishment and grouping

The mice were randomly assigned into 4 groups: the normal, negative control (NC), AIP model and THY1 overexpression groups (12 mice in each group). The model was established using human cytomegalovirus (HCMV) AD169 strain (Tongji University, Shanghai, China). After resuscitation and toxication on human embryo fibroblasts (HF, Anhui Medical University, Hefei, Anhui, China), plaque assay was conducted 3 times for virus purification, and the concentration was

determined. Except those of the normal group, the mice of the other 3 groups were intravenously injected with HCMV strain suspension (6×10^5 plaque forming unit (PFU), about 0.5 mL/mouse) *via* the tail, and the mice in the normal group were injected with an equal amount of normal saline. The activity, diet and existence of shrugged hair of all mice were observed for 3 consecutive days, and the respiratory rate of the mice was examined 1 time each day during the experiment. The serum of the mice was collected on the 3rd day to examine the positive sera rate of HCMV AD169 antibody. Following the examination period, the mice in the ALP model were infected with the concentrated supernatant from packed THY1 lentivirus using nasal intubation drip. Mice in the control group were infected with control lentivirus without THY1 gene. After 7 d, the mice were anesthetized and sacrificed. Some of their lung tissues were fixed in 4% paraformaldehyde and the rest were preserved in 10% formalin for subsequent experiments.

Hematoxylin-eosin (HE) staining

The lung tissues of mice in each group were fixed in 4% paraformaldehyde for more than 24 hours. The tissues were then dehydrated by 70% ethanol for 12 hours, 80% ethanol for 6 hours, 85% ethanol for 1 hour and 90% ethanol for 1 hour. Following that, the tissues were then dehydrated by 95% ethanol for 1 hour, absolute ethanol and regular ethanol for 1 hour each, and then were cleared by xylene I for 20 minutes and xylene II for 20 minutes. After being cleared by xylene II, the tissues were then wax-dipped, paraffin embedded and sliced (4 μm in thickness). After being sliced, the tissues were spread and dried out. The prepared slices were immersed in xylene and dewaxed twice (10 minutes each). Afterwards, the slices were put into ethanol with a concentration gradient of 100%, 95%, 85 and 70% (5 minutes each) and finally rinsed with distilled water before staining. The hematoxylin dye liquor was applied to slices for about 10 minutes, with the excessive dye liquor being washed away with distilled water afterwards. The color separation was conducted using 0.5% ~ 1% hydrochloric acid-ethanol and the reaction was observed under the microscope in order to control the staining process. When the cell nucleus and chromosomes were clear, the slices were rinsed with water for 15 minutes and then stained with 0.1% ~ 0.5% eosin dye liquor for 1 minute, followed by a subsequent water rinse for 1 minute. The slices were dehydrated in ethanol with a concentration gradient of 70%, 80%, 95% and 100% (5 minutes each). The stained slices were cleared twice in xylene I for l0 minutes in total. With the removal of the liquid around the slice using the filter paper, a modest amount of neutral gum was dropped onto the slices. After the slices were mounted with cover glass, the pathological features of lung tissues were observed under an optical microscope.

Masson staining

The specimens were sliced, dewaxed and stained using a Masson staining kit (NanJing JianCheng Bioengineering Institute, Nanjing, China). Before the staining period, the specimens were immersed in distilled water for 30 to 60 seconds, and were then subjected to cell nucleus dye liquor for 4 minutes, followed by rinsing with flushing solution for about 30 seconds, so as to remove excessive dye liquor. Following the removal of the excessive dye liquor, cytoplasmic dye liquor was used to stain cytoplasm for 30 seconds, and the sample was rinsed with flushing solution for 30 seconds to remove excessive dye liquor. With the excessive dye liquor removed, the color separation was performed for 5 to 7 minutes until the significant contrast between the cell nucleus and cytoplasmic fibers was observed under the microscope, indicating that the colors were significantly separated. Finally, the sample was rinsed with absolute ethanol, dried and mounted. The stained collagen fibers in lung tissues were observed under the optical microscope.

Reverse transcription-quantitative polymerase chain reaction (RT-qPCR)

The total cellular RNA was extracted using Trizol (Cat. No.16096020, Thermo Fisher Scientific, NY, USA). The reverse transcription was conducted using 5 μg of RNA to synthesize complementary

DNA (cDNA) templates in accordance with the instructions of the RT kit (Applied Biosystems Inc., Waltham, Massachusetts, USA). The target genes were amplified by PCR with a reaction system of 20 μL, which contained synthesized cDNA (2 μL), forward and reverse primers (0.8 μL each) and UltraSYBR Mixture (10.4 μL). Distilled water was added to reach the total volume of 20 μL and was mixed gently. The reaction conditions were pre-denaturation at 94°C for 5 minutes, followed by 30 cycles of denaturation at 94°C for 30 seconds, annealing at 54.5°C for 30 seconds, and extension at 72°C for 30 seconds, and a final cycle of extension at 72°C for 10 minutes. In order to preserve the products, they were stored at 4°C. The glyceraldehyde-3-phosphate dehydrogenase (GAPDH) was used as the internal reference, and the primer sequences of THY1, matrix metalloproteinase-2 (MMP-2), Occludin, alpha-smooth muscle actin (α-SMA), Vimentin, β-catenin and GAPDH were designed and synthesized by Shanghai Biological Engineering Co., Ltd. (Shanghai, China) (Table 2). The $2^{-\Delta Ct}$ represented the ratio of relative gene expression between the experimental group and the control group. The formula was as follows: $\Delta Ct = Ct_{\text{target gene}} - Ct_{\text{GAPDH}}$. The cycle threshold (Ct) values referred to the amplification cycles when the real-time fluorescence intensity of the reaction reached the set threshold and when the amplification was in the logarithmic growth. Each of these experiments was repeated 3 times.

Table 2. Primer sequences of genes used in reverse transcription-quantitative polymerase chain reaction.

Gene	Primer sequence (5′ – 3′)
THY1	Forward: GCGTCCGAGTACATGGAGA
	Reverse: AAGTCTCTGCGAAGTGTGCTC
MMP-2	Forward: CTATTCTGCCAGCACTTTGG
	Reverse: CAGACTTTGGTTCTCCAACTT
Occludin	Forward: GCTTATCTTGGGAGCCTGGACA
	Reverse: GTCATTGCTTGGTGCATAATGATTG
α-SMA	Forward: GCATCCGACCTTCCTAA
	Reverse: TCTCCAGAGTCCAGCACAATAC
Vimentin	Forward: CGGTTGAGACCAGAGATGGA
	Reverse: TGCTGGTACTGCACTGTTGC
β-catenin	Forward: GAGCCGTCAGTGCAGGAG
	Reverse: CAGCTTGAGTAGCCATTGTCC
GAPDH	Forward: AAATGGTGAAGGTCGGTGTG
	Reverse: TGAAGGGGTCGTTGATGG

THY1, thymocyte differentiation antigen-1; MMP-2, matrix metalloproteinase-2; α-SMA, alpha-smooth muscle actin; GAPDH, glyceraldehyde-3-phosphate dehydrogenase.

Western blot analysis

The left lower lobe of a mouse's lung was obtained and added with tissue radio-immunoprecipitation assay (RIPA) lysate (Shenneng Bocai Biotech Co., Ltd., Shanghai, China). After the tissues were ground into homogenous pulp, the supernatant was extracted through centrifugation to obtain the total protein, and the concentration was determined via Bradford protein detection kit (Shanghai Yeasen Biotech Co., Ltd., Shanghai, China). A fraction of the extracted protein was denatured at 100°C for 5 minutes with loading buffer and stored at −20°C before separation. Total cellular protein (30 μg for each specimen) was separated by sodium dodecyl sulfate-polyacrylamide gel electrophoresis (SDS-PAGE) (100 V, 100 minutes) and then transferred onto the membranes (80 V, 120 minutes). Following the transfer onto the membranes, the membranes were then washed with Tris-buffered saline-Tween (TBST) 3 times (5 minutes per wash), followed by blockade with blocking solution that contained 3% skim milk powder and 0.3% bovine serum albumin (BSA) for 1 hour at room temperature. The membranes were washed again with PBST (PBS containing 0.05% Tween-20) for 5 minutes and incubated at 4°C for one night with the rabbit anti-mouse primary antibodies: THY1 antibody (1: 1000, ab92574), MMP-2 antibody (1: 5000, ab76319), Occludin antibody (1: 5000, ab167161), α-SMA antibody (1: 2000, ab5694), Vimentin antibody (1: 1000, ab92547), p-β-catenin antibody (1: 500, ab75777), and GAPDH antibody (1: 2500, ab9485) (all antibodies were purchased from Abcam, Cambridge, MA, USA). The following day, the membrane was rinsed with PBST 3 times (5 minutes per wash) to remove the excess primary antibodies, followed by an incubation period with the horseradish peroxidase (HRP)-labeled goat anti-rabbit secondary antibody (1: 10000, Abcam, Cambridge, MA, USA) for 1 hour at room temperature. The membranes were once again rinsed with PBST 3 times (5 minutes per wash) prior to film development. Meanwhile, a medium amount of liquid A and liquid B from the electrochemiluminescence (ECL) fluorescence detection kit (Cat. No. BB-3501, AmeNormale, UK) were mixed in a dark

room. The mixture was dropped onto the membranes and then placed in a gel imager for exposure and development. The images were obtained with a Bio-Rad image analysis system (Bio-Rad Laboratories INC., CA, USA) and analyzed using the Quantity One v4.6.2 software. The relative expression of the protein was expressed as the ratio of the gray value of the target protein band to the GAPDH protein band. Each experiment was repeated 3 times.

Insolation, transfection and grouping of mouse lung fibroblasts

The lungs of sacrificed mice were obtained under sterile conditions and the lung tissue was cut into small blocks and dissociated with 0.25% trypsin (Sigma-Aldrich, St. Louis, MO, USA) at 37°C for 30 minutes. After the lung tissue was cut into small blocks, the supernatant was obtained, and an equal volume of RPMI-1640 medium containing 10% fetal bovine serum (FBS) was used to terminate the detachment. The slices were centrifuged at 178 g for 10 minutes and this was done several times. Afterwards, the gathered cells were cultured in RPMI-1640 medium. The dissociated cell suspension was sub-cultured at a ratio of 1: 2, and after 30 minutes, the un-adherent cells were removed. The cells were further cultured in new RPMI-1640 medium until all the cells became fibroblasts. In order to observe the morphological changes, the purified cells were placed under an inverted microscope. The third generation fibroblasts were selected and assigned into 4 groups for transfection. The fibroblasts in the normal and AIP model groups were not transfected with any plasmid, while the fibroblasts in the NC group were transfected with blank plasmids. Meanwhile, the fibroblasts in the THY1 overexpression group were transfected with overexpressed THY1 gene plasmids.

TOP/FOP flash assay

The cells were inoculated into a 96-well plate. After a 24 hour period, cells in each well were added with transfected plasmids, TOP flash or FOP flash, and internal control PRL-TK plasmid (Promega Corporation, Madison, WI, USA) based on the instructions of the lipofectamine 2000 (11668019, Thermo Fisher Scientific, Waltham, MA, USA). The plasmids were then added into a 100 μL L-Dulbecco's modified eagle's medium (DMEM), gently mixed, and allowed to stand at room temperature for 5 minutes. With the removal of the former culture medium, cells were washed with L-DMEM once and transfected with mixed transfection solution for 6 hours, with the medium being replaced with the complete medium. After 24–48 hours of culture, the culture liquid was abandoned. After removal of the liquid culture, the firefly luciferase activity and renilla luciferase activity in each well were detected using the Dual-Luciferase® Reporter Assay System (E1910, Promega Corporation, Madison, WI, USA). The ratio of firefly luciferase activity to renilla luciferase activity referred to the activity of transcription factors of the Wnt/β-catenin signaling pathway [46].

3-(4,5-dimethylthiazol-2-yl)-2,5-diphenyltetrazolium bromide (MTT) assay

The transfected cells were cultured for 24 hours until cells grew by static adherence. When the cell reached approximately 80% confluence, the cells were rinsed twice with PBS and then dissociated into single cell suspension with 0.25% trypsin. Following the cell suspension period, the treated cells were subjected to MTT assay. Each well was replaced with fresh RPMI1640 medium and added with 10% MTT reaction solution (5 g/L, GDY1317, Gudu Biotech Company, Shanghai, China). The cells were dissolved at 37°C for 4 hours to form insoluble purple-blue formazan crystals. The medium was removed and the cells were rinsed with PBS twice. The formazan was then dissolved using dimethyl sulfoxide (DMSO) (150 μL, D5879-100ML, Sigma-Aldrich, St. Louis, MO, USA) and the culture plate was shaken evenly for 5 minutes. The optical density (OD) value of each well was measured at 570 nm (24 hours, 48 hours, and 72 hours) using a microplate reader (Nanjing Defer Laboratory Equipment Co., Ltd., Nanjing, China). Each experiment was repeated 3 times and cell viability curve was drawn with OD values of each group as the ordinate, and time points as the abscissa.

Flow cytometry

Cells that had been transfected for a 48 hour period were dissociated with 0.25% trypsin (ethylenediaminetetraacetic acid (EDTA)-free) (YB15050057, YuBo Company, Shanghai, China) and collected in a flow tube. Afterwards, the centrifugation was conducted and the supernatant was then discarded. The cells were rinsed 3 times with cold PBS and the supernatant was discarded following centrifugation. The Annexin-V-fluorescein isothiocyanate (FITC)/propidium iodide (PI) dye liquor was prepared with Annexin-V-FITC, PI and N-2-hydroxyethylpiperazine-N'-2-ethanesulfonic acid (HEPES) buffer solutions were mixed at a ratio of 1: 2: 50 according to the instructions of Annexin-V-FITC apoptosis detection kit (K201-100, Biovision Inc., Palo Alto, CA, USA). Every 100 μL of dye liquor was used to re-suspend 1×10^6 cells, which were subjected to oscillation, mixing, and incubation at room temperature for 15 minutes, followed by an addition of 1 mL HEPES buffer solution (PB180325, Procell Life Science & Technology Co., Ltd., Wuhan, Hubei, China). Cell apoptosis was analyzed by the detection of FITC and PI fluorescence through activation of band pass at 525 nm and 620 nm respectively by a wavelength of 488 nm. The experiment was repeated 3 times.

Statistical analysis

SPSS 21.0 software (IBM Corp., Armonk, NY, USA) was employed for statistical analysis. The measurement data were displayed as mean ± standard deviation. The *t*-test was utilized for comparison between two groups. Comparisons among multiple groups were performed with one-way analysis of variance, and variance analysis and significance test were conducted. A $p < 0.05$ was considered statistically significant.

Acknowledgments

The authors are grateful to all staff who contributed to this study.

Disclosure statement

No potential conflict of interest was reported by the authors.

References

[1] Larsen BT, Colby TV. Update for pathologists on idiopathic interstitial pneumonias. Arch Pathol Lab Med. 2012;136:1234–1241.
[2] Goncalves-Venade G, Lacerda-Principe N, Roncon-Albuquerque R Jr., et al. Extracorporeal membrane oxygenation for refractory severe respiratory failure in acute interstitial pneumonia. Artif Organs. 2018;42:569–574.
[3] Li H, Zhang J, Song X, et al. Alveolar epithelial cells undergo epithelial-mesenchymal transition in acute interstitial pneumonia: a case report. BMC Pulm Med. 2014;14:67.
[4] Mukhopadhyay S, Parambil JG. Acute interstitial pneumonia (AIP): relationship to Hamman-Rich syndrome, diffuse alveolar damage (DAD), and acute respiratory distress syndrome (ARDS). Semin Respir Crit Care Med. 2012;33:476–485.
[5] Schwanhausser B, Busse D, Li N, et al. Global quantification of mammalian gene expression control. Nature. 2011;473:337–342.
[6] Pei X, Zhu J, Yang R, et al. CD90 and CD24 co-expression is associated with pancreatic intraepithelial neoplasias. PLoS One. 2016;11:e0158021.
[7] Buishand FO, Arkesteijn GJ, Feenstra LR, et al. Identification of CD90 as putative cancer stem cell marker and therapeutic target in insulinomas. Stem Cells Dev. 2016;25:826–835.
[8] Sahin N, Akatli AN, Celik MR, et al. The role of CD90 in the differential diagnosis of pleural malignant mesothelioma, pulmonary carcinoma and comparison with calretinin. Pathol Oncol Res. 2017;23:487–491.
[9] Scognamiglio G, D'Antonio A, Rossi G, et al. CD90 expression in atypical meningiomas and meningioma metastasis. Am J Clin Pathol. 2014;141:841–849.
[10] Schliekelman MJ, Creighton CJ, Baird BN, et al. Thy-1 (+) cancer-associated fibroblasts adversely impact lung cancer prognosis. Sci Rep. 2017;7:6478.
[11] Mesri M, Birse C, Heidbrink J, et al. Identification and characterization of angiogenesis targets through proteomic profiling of endothelial cells in human cancer tissues. PLoS One. 2013;8:e78885.
[12] Chen WC, Hsu HP, Li CY, et al. Cancer stem cell marker CD90 inhibits ovarian cancer formation via beta3 integrin. Int J Oncol. 2016;49:1881–1889.
[13] Kumar A, Bhanja A, Bhattacharyya J, et al. Multiple roles of CD90 in cancer. Tumour Biol. 2016;37:11611–11622.
[14] Chung MT, Liu C, Hyun JS, et al. CD90 (Thy-1)-positive selection enhances osteogenic capacity of human adipose-derived stromal cells. Tissue Eng Part A. 2013;19:989–997.
[15] True LD, Zhang H, Ye M, et al. CD90/THY1 is overexpressed in prostate cancer-associated fibroblasts and could serve as a cancer biomarker. Mod Pathol. 2010;23:1346–1356.

[16] Zhan T, Rindtorff N, Boutros M. Wnt signaling in cancer. Oncogene. 2017;36:1461–1473.
[17] Gurney A, Axelrod F, Bond CJ, et al. Wnt pathway inhibition via the targeting of Frizzled receptors results in decreased growth and tumorigenicity of human tumors. Proc Natl Acad Sci U S A. 2012;109:11717–11722.
[18] Skronska-Wasek W, Gosens R, Konigshoff M, et al. WNT receptor signalling in lung physiology and pathology. Pharmacol Ther. 2018;187:150–166.
[19] Li ZQ, Ding W, Sun SJ, et al. Cyr61/CCN1 is regulated by Wnt/beta-catenin signaling and plays an important role in the progression of hepatocellular carcinoma. PLoS One. 2012;7:e35754.
[20] Chen WJ, Ho CC, Chang YL, et al. Cancer-associated fibroblasts regulate the plasticity of lung cancer stemness via paracrine signalling. Nat Commun. 2014;5:3472.
[21] Akhmetshina A, Palumbo K, Dees C, et al. Activation of canonical Wnt signalling is required for TGF-beta-mediated fibrosis. Nat Commun. 2012;3:735.
[22] Salim MU, Mustahsan SM, Fatima A. Abruptio placentae with type II respiratory failure secondary to acute interstitial pneumonia responsive to steroids. J Coll Physicians Surg Pak. 2017;27:S106–S7.
[23] Cosgrove GP, Bianchi P, Danese S, et al. Barriers to timely diagnosis of interstitial lung disease in the real world: the INTENSITY survey. BMC Pulm Med. 2018;18:9.
[24] Huang K, Kang X, Wang X, et al. Conversion of bone marrow mesenchymal stem cells into type II alveolar epithelial cells reduces pulmonary fibrosis by decreasing oxidative stress in rats. Mol Med Rep. 2015;11:1685–1692.
[25] Yang IV. Epigenomics of idiopathic pulmonary fibrosis. Epigenomics. 2012;4:195–203.
[26] Chang Y, Li C, Jia Y, et al. CD90(+) cardiac fibroblasts reduce fibrosis of acute myocardial injury in rats. Int J Biochem Cell Biol. 2018;96:20–28.
[27] Fernandez IE, Eickelberg O. New cellular and molecular mechanisms of lung injury and fibrosis in idiopathic pulmonary fibrosis. Lancet. 2012;380:680–688.
[28] Distler A, Deloch L, Huang J, et al. Inactivation of tankyrases reduces experimental fibrosis by inhibiting canonical Wnt signalling. Ann Rheum Dis. 2013;72:1575–1580.
[29] Vancheri C. Common pathways in idiopathic pulmonary fibrosis and cancer. Eur Respir Rev. 2013;22:265–272.
[30] Piersma B, Bank RA, Boersema M. Signaling in Fibrosis: TGF-beta, WNT, and YAP/TAZ Converge. Front Med (Lausanne). 2015;2:59.
[31] Kim TH, Kim SH, Seo JY, et al. Blockade of the Wnt/beta-catenin pathway attenuates bleomycin-induced pulmonary fibrosis. Tohoku J Exp Med. 2011;223:45–54.
[32] Lee H, Kang J, Lee J. Involvement of YAP-1, the homolog of yes-associated protein, in the Wnt-mediated neuronal polarization in caenorhabditis elegans. G3 (Bethesda). 2018;8:2595–2602.
[33] Ou C, Sun Z, Li S, et al. Dual roles of yes-associated protein (YAP) in colorectal cancer. Oncotarget. 2017;8:75727–75741.
[34] Kim NH, Lee Y, Yook JI. Dishevelling Wnt and Hippo. BMB Rep. 2018;51:425–426.
[35] Sulaiman A, McGarry S, Li L, et al. Dual inhibition of Wnt and Yes-associated protein signaling retards the growth of triple-negative breast cancer in both mesenchymal and epithelial states. Mol Oncol. 2018;12:423–440.
[36] Record M. Intercellular communication by exosomes in placenta: a possible role in cell fusion? Placenta. 2014;35:297–302.
[37] Hu Y, Yan C, Mu L, et al. Fibroblast-derived exosomes contribute to chemoresistance through priming cancer stem cells in colorectal cancer. PLoS One. 2015;10:e0125625.
[38] Ni J, Li H, Zhou Y, et al. Therapeutic potential of human adipose-derived stem cell exosomes in stress urinary incontinence - an in vitro and in vivo study. Cell Physiol Biochem. 2018;48:1710–1722.
[39] Qin LH, Huang W, Mo XA, et al. LPS induces occludin dysregulation in cerebral microvascular endothelial cells via MAPK signaling and augmenting MMP-2 levels. Oxid Med Cell Longev. 2015;2015:120641.
[40] Wang D, Wang D, Wang N, et al. Long non-coding RNA BANCR promotes endometrial cancer cell proliferation and invasion by regulating MMP2 and MMP1 via ERK/MAPK signaling pathway. Cell Physiol Biochem. 2016;40:644–656.
[41] He J, Liu Y, Zhu T, et al. CD90 is identified as a candidate marker for cancer stem cells in primary high-grade gliomas using tissue microarrays. Mol Cell Proteomics. 2012;11:M111 010744.
[42] Parry PV, Engh JA. CD90 is identified as a marker for cancer stem cells in high-grade gliomas using tissue microarrays. Neurosurgery. 2012;70:N23–N24.
[43] Rege TA, Hagood JS. Thy-1, a versatile modulator of signaling affecting cellular adhesion, proliferation, survival, and cytokine/growth factor responses. Biochim Biophys Acta. 2006;1763:991–999.
[44] Xing S, Nie F, Xu Q, et al. HDAC is essential for epigenetic regulation of Thy-1 gene expression during LPS/TLR4-mediated proliferation of lung fibroblasts. Lab Invest. 2015;95:1105–1116.
[45] Liu X, Wong SS, Taype CA, et al. Thy-1 interaction with Fas in lipid rafts regulates fibroblast apoptosis and lung injury resolution. Lab Invest. 2017;97:256–267.
[46] Yu B, Ye X, Du Q, et al. The long non-coding RNA CRNDE promotes colorectal carcinoma progression by competitively binding miR-217 with TCF7L2 and enhancing the Wnt/beta-catenin signaling pathway. Cell Physiol Biochem. 2017;41:2489–2502.